AGU PUBLICATIONS

Geophysical Research Letters

RESEARCH LETTER
10.1002/2015GL065562

Key Points:
- New airborne in situ ozone data over tropical western Pacific from surface to 15 km
- Data show a dominant feature in ozone distribution near 20 ppbv throughout the troposphere
- A secondary mode near 60 ppbv is formed by O_3-enhanced and H_2O-reduced air masses

Correspondence to:
L. L. Pan,
liwen@ucar.edu

Citation:
Pan, L. L., et al. (2015), Bimodal distribution of free tropospheric ozone over the tropical western Pacific revealed by airborne observations, *Geophys. Res. Lett.*, *42*, doi:10.1002/2015GL065562.

Received 27 JUL 2015
Accepted 27 AUG 2015
Accepted article online 1 SEP 2015

Bimodal distribution of free tropospheric ozone over the tropical western Pacific revealed by airborne observations

L. L. Pan[1], S. B. Honomichl[1], W. J. Randel[1], E. C. Apel[1], E. L. Atlas[2], S. P. Beaton[1], J. F. Bresch[1], R. Hornbrook[1], D. E. Kinnison[1], J.-F. Lamarque[1], A. Saiz-Lopez[3], R. J. Salawitch[4], and A. J. Weinheimer[1]

[1]National Center for Atmospheric Research, Boulder, Colorado, USA, [2]Department of Atmospheric Sciences, RSMAS, University of Miami, Miami, Florida, USA, [3]Atmospheric Chemistry and Climate Group, Institute of Physical Chemistry Rocasolano, CSIC, Madrid, Spain, [4]Department of Atmospheric and Oceanic Science, Department of Chemistry and Biochemistry, and Earth System Science Interdisciplinary Center, University of Maryland, College Park, Maryland, USA

Abstract A recent airborne field campaign over the remote western Pacific obtained the first intensive in situ ozone sampling over the warm pool region from oceanic surface to 15 km altitude (near 360 K potential temperature level). The new data set quantifies ozone in the tropical tropopause layer under significant influence of convective outflow. The analysis further reveals a bimodal distribution of free tropospheric ozone mixing ratio. A primary mode, narrowly distributed around 20 ppbv, dominates the troposphere from the surface to 15 km. A secondary mode, broadly distributed with a 60 ppbv modal value, is prominent between 3 and 8 km (320 K to 340 K potential temperature levels). The latter mode occurs as persistent layers of ozone-rich drier air and is characterized by relative humidity under 45%. Possible controlling mechanisms are discussed. These findings provide new insight into the physical interpretation of the "S"-shaped mean ozone profiles in the tropics.

1. Introduction

Tropospheric ozone plays an important role in atmospheric chemistry and climate forcing. Ozone controls the atmospheric oxidizing capacity via its photochemical link to OH [*Brasseur et al.*, 1999], and this link is especially important in the moist, high-radiation environment of the tropics. Tropospheric ozone is also a significant greenhouse gas, and its contribution to the radiative forcing of climate change continues to have significant uncertainty [*Intergovernmental Panel on Climate Change*, 2013]. Understanding the behavior of tropical ozone and its controlling mechanisms is a key aspect of evaluating and improving chemistry-climate models.

In this letter, we report new observations and analyses of the tropospheric ozone profiles in the remote tropical western Pacific (TWP) obtained from a recent airborne campaign, Convective Transport of Active Species in the Tropics (CONTRAST). The CONTRAST experiment was conducted from Guam (13.5°N, 144.8°E) using the National Science Foundation/National Center for Atmospheric Research (NSF/NCAR) Gulfstream V (GV) research aircraft during January and February 2014. CONTRAST was one of the three coordinated airborne experiments to investigate the impact of deep convection and convective transport on atmospheric composition from the ocean surface to the lower stratosphere during the Northern Hemisphere winter over the TWP, where the most extensive and persistent deep convection in Earth's climate system occurs. The partner experiments were Airborne Tropical Tropopause Experiment, which deployed the high-altitude NASA Global Hawk, and Coordinated Airborne Studies in the Tropics, which used the UK FAAM BAe 146 research aircraft. A total of 16 research flights were conducted during CONTRAST using the GV, with measurements of O_3, H_2O, and a large suite of additional chemical tracers. The research flights from Guam covered 20°S to 40°N latitude, 130°E to 165°E longitude. Nearly 100 vertical profiles were sampled between the marine boundary layer (near 0.1 km above sea level, asl) and the upper troposphere (up to 15.2 km asl, potential temperature level ~360 K). These data represent the most intensive sampling of atmospheric composition over the TWP during boreal winter and the only high-resolution in situ profile measurements up to 15 km in the region.

One of the main objectives of the CONTRAST campaign was to investigate the impact of deep convection on chemical composition and the ozone photochemical budget in the tropical atmosphere. Previous ozone measurements over the remote tropical Pacific have been mainly provided by ozonesonde including the

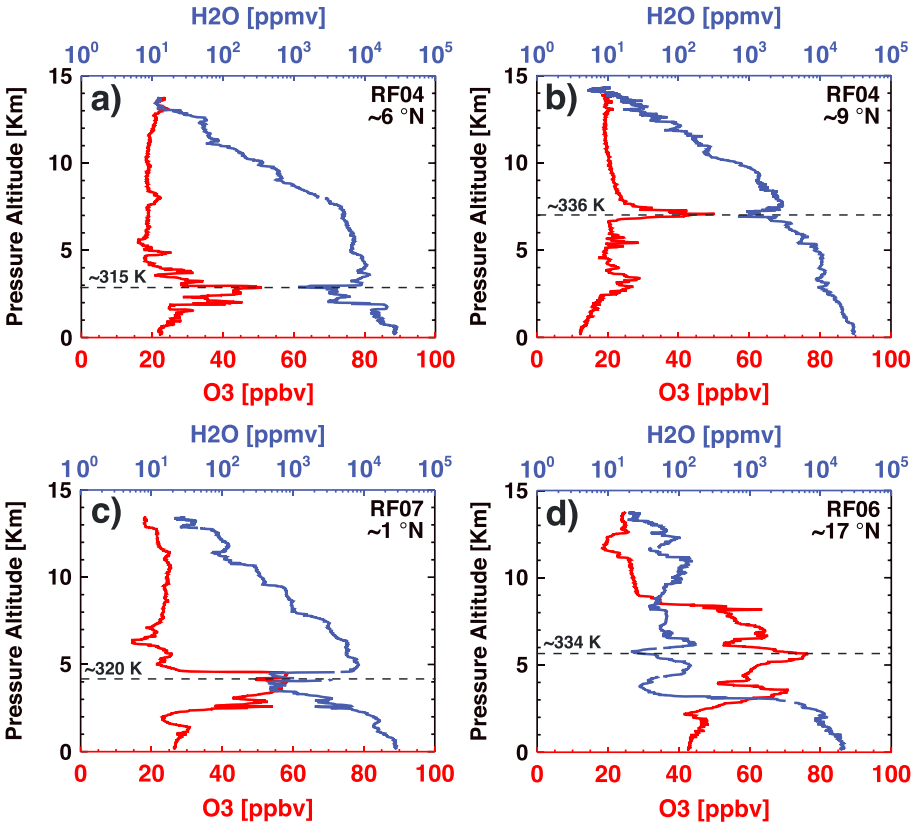

Figure 1. Examples of O_3 and H_2O profiles with anticorrelated layers. A selected potential temperature level is shown in each case to give some indications of the vertical location of the layers in potential temperature.

Southern Hemisphere Additional Ozonesonde (SHADOZ) network [*Oltmans et al.*, 2001; *Thompson et al.*, 2011]. Ozonesondes from research vessels have provided vertical profile measurements for a limited number of projects, including the Central Equatorial Pacific Experiment (March–April 1993) [*Kley et al.*, 1997] and the TransBrom mission [*Rex et al.*, 2014]. The TWP region was also investigated during NASA Pacific Exploratory Mission experiments and the Transport and Chemical Evolution over the Pacific experiment, where extensive in situ measurements over the western and central tropical Pacific region were made using the DC-8 research aircraft up to 12 km [*Crawford et al.*, 1997; *Hoell et al.*, 1999; *Stoller et al.*, 1999; *Jacob et al.*, 2003]. Also, the Biomass Burning and Lightning Experiment obtained in situ ozone in the TWP region up to 13.5 km during August–October 1998 and 1999 using a G-II aircraft [*Kondo et al.*, 2002]. Hence, previous airborne in situ data did not provide information for the tropical tropopause layer (TTL), which spans from the outflow of convection (~13 km) to the base of the lower stratosphere (~17 km) [e.g., *Gettelman and Forster*, 2002; *Fueglistaler et al.*, 2009; *Pan et al.*, 2014].

Ozone variability over the TWP warm pool, especially the influence of deep convective outflow on ozone concentration in the TTL, has become a topic of renewed interest following ozonesonde measurements in this region that showed cases of extremely low ozone, below ozonesonde detection limit of 15 ppbv, between 12 and 15 km altitudes [*Rex et al.*, 2014]. These results led to a hypothesis of corresponding regional OH minimum. In this letter we present the first high-accuracy and low detection limit in situ ozone measurements up to 15 km in the core of the TWP warm pool region. Characterization of the ozone distribution and its close relationship with water vapor are the main focus of this letter.

2. In Situ Ozone and Water Vapor Measurements During CONTRAST

The in situ O_3 measurements on the GV were made using the NCAR chemiluminescence instrument [*Ridley et al.*, 1992]. The accuracy of the O_3 mixing ratio is estimated to be within 5% for the entire range of ozone measurements during CONTRAST. The detection limit is 0.1 ppbv at 1 s sampling rate at high altitude. In situ water vapor

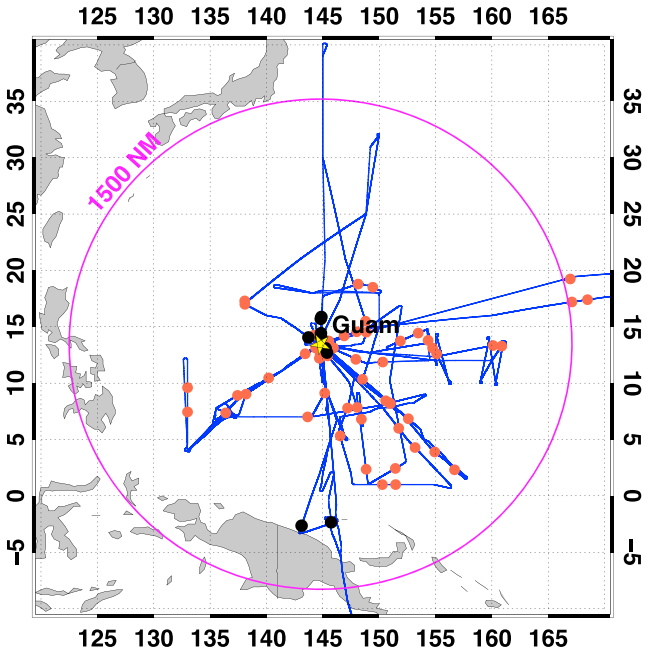

Figure 2. CONTRAST GV flight tracks (blue lines) in the TWP domain and locations of profiles (dots). A total of 85 profiles that include sampling of the midtroposphere are shown. Profiles with anticorrelated O_3 and H_2O layers are shown in red (76 profiles), and those without are shown in black (nine cases). The magenta circle shows the nominal GV round-trip range from Guam.

measurements were made using the vertical cavity surface emitting laser hygrometer [*Zondlo et al.*, 2010]. The accuracy of water vapor mixing ratio is estimated to be within 6% for the range of measurements during CONTRAST. Data for the CONTRAST experiment are reported at 1 Hz. At this sampling rate with typical air speed and vertical climb rates of the GV, the spatial resolution is approximately 200 m horizontally and ~7 m vertically during climbs and descents. The results reported in this letter are largely based on vertical profiles.

Throughout the experiment, the GV flights were designed to evaluate the distribution of trace gases under different meteorological conditions, especially the vertical structure of convectively influenced air masses. Vertical profiles were sampled mostly using en route flight patterns, although spiral profiling was done for isolated cases. A ubiquitous feature of these profiles was the enhancement of ozone in layer structures, frequently anticorrelated with the water vapor. Figure 1 shows four selected examples of these profiles. As shown, the vertical depth of the layers varies from a few hundred meters to a couple of kilometers. The altitude of the layers ranges from around 2 km asl, which was often near the top of the trade wind inversion, to approximately 9 km.

The locations of the ozone-enhanced layers sampled by the GV are shown in Figure 2, which highlights the ubiquitous nature of these layers during the experiment. Among the total of 85 profiles sampled in the TWP region, 76 of them exhibit anticorrelated layer structure (red) while nine lack such structures (black). The anticorrelation identification is based on the joint condition of relative humidity (RH) less than 45% and ozone mixing ratio greater than 30 ppbv in the pressure range 900 to 300 hPa, rather than correlation of detailed profile structure.

Note that the layered structures in the tropical troposphere have been documented using DC-8 in situ measurements and ozonesonde data [e.g., *Stoller et al.*, 1999; *Thouret et al.*, 2001; *Hayashi et al.*, 2008]. The previous analyses, however, focused on detailed structural correlation in the profiles. The high sampling density and the different analyses approach we present in this work reveal a fundamental bimodal distribution of tropical tropospheric ozone.

3. Quantification of TTL Ozone and a Bimodal Distribution of Midtropospheric Ozone

Figure 3 shows the vertical structure of the ozone distribution using all GV profiles within the TWP domain (5°S–20°N, 130°E–170°E). Figures 3a and 3b show "layer-normalized" relative frequency distributions of ozone and water vapor, respectively, in GPS altitude for the full range of the GV measurements. The density indicates that the dominant feature of the ozone distribution is a near-constant mixing ratio of about 20 ppbv throughout the troposphere. It also indicates that most of the ozone enhancements occur between 2 and 9 km in altitude (approximately 315–345 K in potential temperature). On the other hand, the water vapor distribution shows the high-density distribution between 45 and 100% RH. The histogram

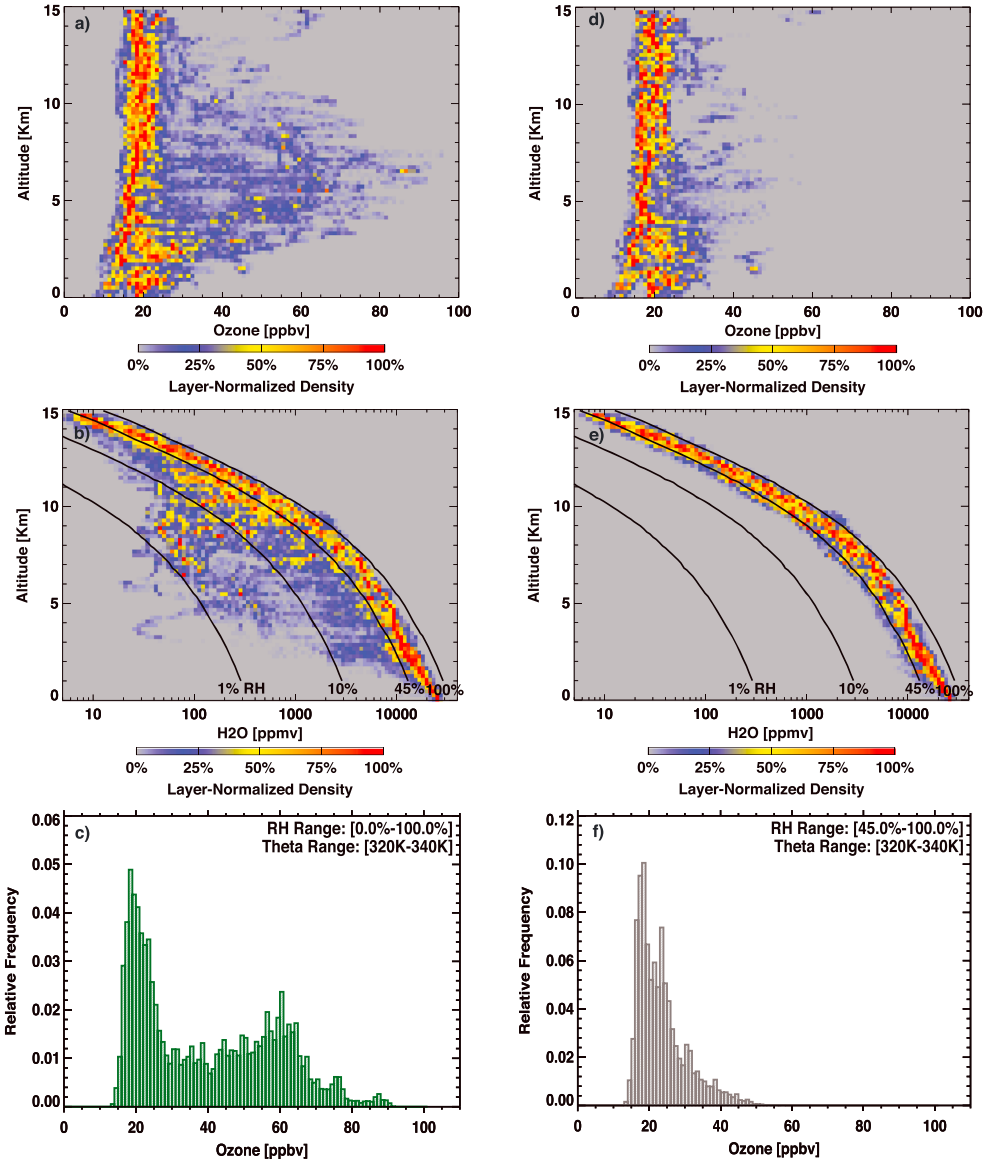

Figure 3. Relative frequency distribution (with respect to the layer maximum) from all GV TWP (a) ozone and (b) water vapor profiles in altitude (200 m interval) and selected RH profiles in GPS altitude coordinates and (c) the relative frequency distribution of ozone from 320 to 340 K potential temperature layer. (d–f) The same as Figures 3a–3c respectively but with measurements less than 45% RH excluded.

of the relative frequency of all ozone observations in the enhanced layer is shown in Figure 3c, highlighting a bimodal distribution. The modal value of the "primary mode" is 18 ppbv, and the distribution of this mode is fairly narrow, ±5 ppbv. The secondary mode is characterized by a broad distribution from ~35 ppbv to 95 ppbv, with the modal value near 60 ppbv.

Figures 3d and 3e show the layer-normalized relative frequencies of ozone and water vapor excluding data with RH less than 45% (calculated using colocated water vapor and temperature measurements). Similarly, Figure 3f is the counterpart of Figure 3c with <45% RH samples excluded and shows that the secondary mode (measurements of enhanced ozone) no longer appears in the distribution. Note that the less than 45% RH condition also excludes a fraction of the upper tropospheric air masses in the primary mode, mostly from 9 km and above. The 45% RH criterion was chosen to isolate the secondary mode with minimum impact on the upper tropospheric samples in the primary mode.

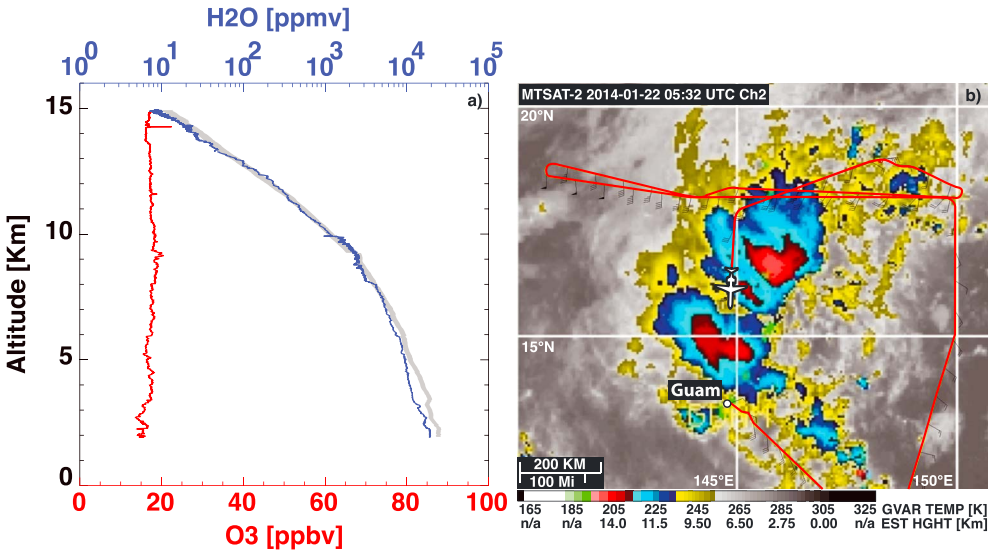

Figure 4. (a) Convectively controlled O_3 and H_2O profiles sampled during research flight on 22 January 2014 in a profile from ~2 km to ~15 km asl, approximately 2° north of Guam. The gray curve shows the calculated saturation mixing ratio (with respect to liquid water below and to ice above 400 hPa) using the measured temperature. The width of the gray curve indicates the impact of a ±1° uncertainty of temperature data. The close alignment of water vapor and saturation vapor profiles indicates saturation with respect to ice above ~8 km (~400 hPa). (b) The spiral ascent was conducted near two mature deep convective systems, as indicated by the satellite image and the aircraft icon. The satellite IR temperature field indicates that the convective top was near 15 km altitude. The red line shows the GV flight track prior to the profiling.

Overall, Figure 3 shows that the primary mode near 20 ppbv of ozone dominates the entire troposphere over the TWP during this season. The figure also reveals that the ozone-enhanced secondary mode is entirely associated with air drier than 45% RH. Note that the distributions show in Figure 3 are a result of sampling under the full range of conditions over TWP, including background conditions without immediate convection, as well as both fresh and aged convective outflow.

From the extensive GV sampling, the lowest ozone mixing ratio is 13 ppbv in the 12–15 km altitude range. In addition, the GV made collocated flights with ozonesonde launches over Manus Island (~2°N, 147°E) during the campaign, leading to improved understanding of ozonesonde background current calibration issues [*Newton et al.*, 2015].

4. Possible Controlling Mechanisms

The CONTRAST profile measurements suggest that the primary ozone mode reflects background conditions of the tropical troposphere and is largely controlled by the vertical redistribution of near-surface ozone concentration by convective processes in balance with photochemical ozone production and destruction processes. A specific example is given in Figure 4, which shows the O_3, H_2O, and saturation vapor (calculated from the GV temperature measurement) profiles observed in a spiral ascent (Figure 4a) between two deep convective towers (Figure 4b), during the research flight on 22 January. This case provides an excellent isolated example of the unperturbed primary mode profiles—where the O_3 mixing ratio is nearly constant (~15–20 ppbv) with respect to altitude. The water vapor profile is saturated with respect to ice above 400 hPa (~8 km) with subsaturated layers below 400 hPa consistent with a precipitating downdraft [*Zipser*, 1977] that is further evidence of vertical mixing in this case. This case suggests that tropical convective overturning homogenizes the air mass leaving behind a column devoid of sharp ozone-rich dry layers throughout the troposphere. The hypothesis that this process creates and maintains the primary mode is consistent with all TWP GV observations, since the water vapor profiles in the primary mode are all near saturation in the midtroposphere. This hypothesis is also consistent with the tracer information, which will be analyzed in follow-up studies.

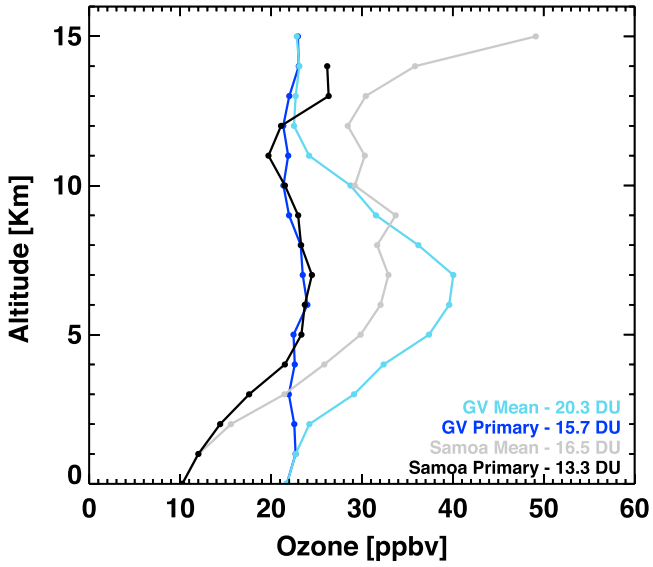

Figure 5. Mean profiles of CONTRAST GV ozone and the mean of the primary mode compared to mean and primary mode profiles from Samoa ozonesonde data in DJF season (141 profiles). The total ozone (in DU) from surface to 14 km is calculated for each mean profile.

The dynamical and chemical mechanisms that control the midtropospheric enhanced ozone mode are under investigation. The mechanisms involved will need to explain three key characteristics of this mode: (a) the ozone enhancement, (b) anomalously dry air masses, and (c) the occurrence of vertical layers of variable depth occurring at levels between 315 and 345 K (and not above).

Independent of ozone measurement, there have been extensive studies of dry layers in the tropics (also known as "dry intrusions"), largely motivated by the observations in the tropical Pacific during the Tropical Ocean–Global Atmosphere Coupled Ocean-Atmosphere Response Experiment field campaign [e.g., *Parsons et al.*, 1994; *Mapes and Zuidema*, 1996]. The dry intrusions were proposed to result from horizontal advection of air from the extratropical tropopause region, in many cases with descent following large-scale Rossby wave breaking events [e.g., *Yoneyama and Parsons*, 1999; *Cau et al.*, 2005, 2007]. Such an origin is consistent with air being dry and ozone rich.

Using back trajectory analyses, *Hayashi et al.* [2008] concluded that transport from the midlatitude upper troposphere/lower stratosphere made a significant contribution to ozone-enhanced layers observed in tropical ozonesonde data. These analyses all suggest that the secondary mode is controlled by nonlocal processes.

An additional mechanism that may contribute to the ozone enhancement is photochemical production of ozone in air masses influenced by biomass burning. This mechanism has been investigated in previous studies and has been shown to contribute to elevated tropical tropospheric ozone levels [e.g., *Gregory et al.*, 1999; *Kita et al.*, 2000; *Kondo et al.*, 2002]. CONTRAST measurements of chemical composition (including HCN and CH_3CN) also indicate the likely contribution of biomass burning emissions to the enhanced ozone layers. This mechanism alone, however, does not necessarily explain the strong anticorrelation with water vapor in the observed layers. We hypothesize that mixing of biomass burning emissions into the large-scale flow along the equatorward flank of the subtropical jet may help explain the key characteristics of the secondary ozone mode.

5. Implications of the Bimodal Structure

Mean profiles from ozonesonde data are often used to evaluate models [e.g., *Saiz-Lopez et al.*, 2012]. The bimodal structure of the ozone distribution suggests that the mean profiles do not adequately represent the major processes that control tropical ozone. Figure 5 shows that the maximum of the mean profile from the CONTRAST GV data is approximately 40 ppbv, a value that is least likely to occur (see Figure 3c) and results from averaging the two modes. Figure 5 also shows the mean profile of the primary mode, which is approximately 20 ppbv throughout the troposphere and represents the TWP ozone profile without the influence of the nonlocal processes. To explore whether similar behavior exists in ozonesonde data, we also show a similar pair of profiles derived from SHADOZ Samoa (14.2°S, 170.6°W) measurements for the December-January-February (DJF) season. Samoa is located at the edge of the TWP warm pool with cleaner southern hemispheric boundary conditions. These varying conditions are responsible for the difference in the mean profiles in the lower levels up to 3 km and the TTL. The midtropospheric ozone distribution, however, is very similar to the GV profiles, with a mean tropospheric maximum near 33 ppbv and a mean primary mode (also identified by excluding 45% RH data) near 20 ppbv. In the 320–340 K layer (3–8 km), the Samoa data show similar behavior to that in Figures 3c and 3d.

The two pairs of mean profiles are also used to estimate the impact of the nonlocal processes on tropical tropospheric total ozone. The results, as given in Figure 5, show that the secondary mode increases total ozone by approximately 20–25%.

The vertical structure of mean tropical tropospheric ozone profiles from ozonesonde data across the stations in the tropics is similar to the Samoa mean profile, with low near-surface values, enhancements in the middle troposphere, low values in the upper troposphere, and rapid increases in the stratosphere [e.g., *Oltmans et al*., 2001]. This structure, often referred to as "S" shaped [e.g., *Folkins et al*., 2002], has been interpreted as mainly controlled by convection, and the upper tropospheric minimum around 345–355 K (~12–14 km) has been considered as an indication of the level of main convective outflow. The new GV observations suggest a possible different interpretation, with a convectively controlled ozone profile throughout the troposphere (maintaining ozone ~20 ppbv up to 15 km or 360 K over TWP) and layered enhancements in the middle troposphere controlled by other, nonlocal processes. In this case the S-shaped structure is largely created by midtroposphere enhancements, not convective outflow of low ozone in the upper troposphere. The minimum in mean ozone profile near 12 km (~345 K) reflects the diminished influence of the secondary mode at these altitudes.

6. Summary and Conclusions

The high-resolution, high-accuracy in situ ozone measurements during CONTRAST provide significant new quantification of the TTL ozone variability over the TWP. The GV flight ceiling of 15 km asl enabled in situ ozone profiles above the sampling range of past airborne experiments in the region. From the extensive GV sampling, no case of near-zero ozone, as have been reported from ozonesondes (which has a detection limit near 15 ppbv) [e.g., *Kley et al*., 1996; *Rex et al*., 2014], was found during the experiment.

CONTRAST observations reveal a bimodal distribution of tropospheric ozone in the TWP, with the modes separated according to (1) nearly constant O_3 values throughout the troposphere (~20 ppbv) associated with near-saturated water vapor profile (primary mode) and (2) enhanced ozone (~35–95 ppbv) and depressed water vapor (secondary mode). The primary mode is consistent with convectively mixed near-surface ozone values. The secondary mode occurs primarily in horizontal layered structures over ~320–340 K and is consistent with advection and mixing from outside of the deep tropics. Although anticorrelated layers of high ozone and low water vapor have been observed previously, analyses focused on details of the vertical profiles and frequency of occurrence of the anticorrelated layers [e.g., *Stoller et al*., 1999; *Thouret et al*., 2001; *Hayashi et al*., 2008]. Our data and analysis lead to a new conclusion that the ozone-enhanced layers form a secondary mode and the $<45\%$ RH condition describes the entire population of this mode regardless of the details of the layer structure.

The recognition of the bimodal structure is important because the different controlling mechanisms behind each mode may behave differently in model simulations, and they may evolve differently in a changing climate. It is, therefore, important for the chemistry-climate models to represent the processes that produced the bimodal distribution.

The CONTRAST data provide additional insight regarding interpretation of the tropical tropospheric ozone structure. Our analysis reveals that the S-shaped mean tropical tropospheric ozone profile is a result of averaging two modes. The ozone-enhanced dry layers play a significant role in creating the S-shaped structure.

Acknowledgments

Funding for this work was provided by the National Science Foundation (NSF) via its sponsorship of the National Center for Atmospheric Research (NCAR). The CONTRAST experiment was funded by NSF. We thank the pilots and the NCAR research aviation facility staff for the successful flight operation. E.A. and R.J.S. acknowledge support from NSF Atmospheric Chemistry Program. The CONTRAST data are available to the public and can be accessed at http://data.eol.ucar.edu/master_list/?project=CONTRAST.

The Editor thanks two anonymous reviewers for their assistance in evaluating this paper.

References

Brasseur, G. P., J. Orlando, and G. Tyndall (1999), *Atmospheric Chemistry and Global Change*, 654 pp., Oxford Univ. Press, New York.

Cau, P., J. Methven, and B. Hoskins (2005), Representation of dry tropical layers and their origins in ERA-40 data, *J. Geophys. Res.*, *110*, D06110, doi:10.1029/2004JD004928.

Cau, P., J. Methven, and B. Hoskins (2007), Origins of dry air in the tropics and subtropics, *J. Clim.*, *20*(12), 2745–2759, doi:10.1175/JCLI4176.

Crawford, J. H., et al. (1997), Implications of large scale shifts in tropospheric NO_x levels in the remote tropical Pacific, *J. Geophys. Res.*, *102*, 28,447–28,468, doi:10.1029/97JD00011.

Folkins, I., C. Braun, A. M. Thompson, and J. Witte (2002), Tropical ozone as an indicator of deep convection, *J. Geophys. Res.*, *107*(D13), 4184, doi:10.1029/2001JD001178.

Fueglistaler, S., A. E. Dessler, T. J. Dunkerton, I. Folkins, Q. Fu, and P. W. Mote (2009), Tropical tropopause layer, *Rev. Geophys.*, *47*, RG1004, doi:10.1029/2008RG000267.

Gettelman, A., and P. M. d. F. Forster (2002), A climatology of the tropical tropopause layer, *J. Meteorol. Soc. Jpn.*, *80*, 911–942.

Gregory, G. L., et al. (1999), Chemical characteristics of Pacific tropospheric air in the region of the Intertropical Convergence Zone and South Pacific Convergence Zone, *J. Geophys. Res.*, *104*, 5677–5696, doi:10.1029/98JD01357.

Hayashi, H., K. Kita, and S. Taguchi (2008), Ozone-enhanced layers in the troposphere over the equatorial Pacific Ocean and the influence of transport of midlatitude UT/LS air, *Atmos. Chem. Phys.*, *8*, 2609–2621, doi:10.5194/acp-8-2609-2008.

Hoell, J. M., D. D. Davis, D. J. Jacob, M. O. Rodgers, R. E. Newell, H. E. Fuelberg, R. J. McNeal, J. L. Raper, and R. J. Bendura (1999), Pacific Exploratory Mission in the tropical Pacific: PEM-Tropics A, August–September 1996, *J. Geophys. Res.*, *104*, 5567–5583, doi:10.1029/1998JD100074.

Intergovernmental Panel on Climate Change (2013), *Climate Change 2013: The Physical Science Basis. Contribution of Working Group I to the Fifth Assessment Report of the Intergovernmental Panel on Climate Change*, edited by T. F. Stocker et al., 1535 pp., Cambridge Univ. Press, Cambridge, U. K., and New York.

Jacob, D. J., J. H. Crawford, M. M. Kleb, V. S. Connors, R. J. Bendura, J. L. Raper, G. W. Sachse, J. C. Gille, L. Emmons, and C. L. Heald (2003), The Transport and Chemical Evolution over the Pacific (TRACE-P) aircraft mission: Design, execution, and first results, *J. Geophys. Res.*, *108*(D20), 9000, doi:10.1029/2002JD003276.

Kita, K., M. Fujiwara, and S. Kawakami (2000), Total ozone increase associated with forest fires over the Indonesian region and its relation to the El Niño-Southern Oscillation, *Atmos. Environ.*, *34*, 2681–2690.

Kley, D., P. J. Crutzen, H. G. J. Smit, H. Vömel, S. J. Oltmans, H. Grassl, and V. Ramanathan (1996), Observations of near-zero ozone concentrations over the convective Pacific: Effects on air chemistry, *Science*, *274*, 230–233, doi:10.1126/science.274.5285.230.

Kley, D., H. G. J. Smit, H. Vömel, H. Grassl, V. Ramanathan, P. J. Crutzen, S. Williams, J. Meywerk, and S. J. Oltmans (1997), Tropospheric water vapour and ozone cross sections in a zonal plane over the central equatorial Pacific, *Q. J. R. Meteorol. Soc.*, *123*, 2009–2040.

Kondo, Y., et al. (2002), Effects of biomass burning, lightning, and convection on O_3, CO, and NO_y over the tropical Pacific and Australia in August–October 1998 and 1999, *J. Geophys. Res.*, *107*(D3), 8402, doi:10.1029/2001JD000820, [printed 108(D3), 2003]

Mapes, B. E., and P. Zuidema (1996), Radiative-dynamical consequences of dry tongues in the tropical troposphere, *J. Atmos. Sci.*, *53*, 620–638.

Newton, R., G. Vaughan, H. M. A. Ricketts, L. L. Pan, A. J. Weinheimer, and C. Chemel (2015), Ozonesonde profiles from the West Pacific Warm Pool, *Atmos. Chem. Phys. Discuss.*, *15*, 16,655–16,696, doi:10.5194/acpd-15-16655-2015.

Oltmans, S. J., et al. (2001), Ozone in the Pacific tropical troposphere from ozonesonde observations, *J. Geophys. Res.*, *106*, 32,503–32,525, doi:10.1029/2000JD900834.

Pan, L. L., L. C. Paulik, S. B. Honomichl, L. A. Munchak, J. Bian, H. B. Selkirk, and H. Vömel (2014), Identification of the tropical tropopause transition layer using the ozone-water vapor relationship, *J. Geophys. Res. Atmos.*, *119*, 3586–3599, doi:10.1002/2013JD020558.

Parsons, D., et al. (1994), The Integrated Sounding System: Description and preliminary observations from TOGA COARE, *Bull. Am. Meteorol. Soc.*, *75*, 553–567.

Rex, M., et al. (2014), A tropical West Pacific OH minimum and implications for stratospheric composition, *Atmos. Chem. Phys.*, *14*, 4827–4841, doi:10.5194/acp-14-4827-2014.

Ridley, B. A., F. E. Grahek, and J. G. Walega (1992), A small, high-sensitivity, medium-response ozone detector for measurements from light aircraft, *J. Atmos. Oceanic Technol.*, *9*, 142–148.

Saiz-Lopez, A., et al. (2012), Estimating the climate significance of halogen-driven ozone loss in the tropical marine troposphere, *Atmos. Chem. Phys.*, *12*, 3939–3949, doi:10.5194/acp-12-3939-2012.

Stoller, P., et al. (1999), Measurements of atmospheric layers from the NASA DC-8 and P-3B aircraft during PEM-Tropics A, *J. Geophys. Res.*, *104*, 5745–5764, doi:10.1029/98JD02717.

Thompson, A. M., S. J. Oltmans, D. W. Tarasick, P. von der Gathen, H. G. J. Smit, and J. C. Witte (2011), Strategic ozone sounding networks: Review of design and accomplishments, *Atmos. Environ.*, *45*(13), 2145–2163.

Thouret, V., J. Y. N. Cho, M. J. Evans, R. E. Newell, M. A. Avery, J. D. W. Barrick, G. W. Sachse, and G. L. Gregory (2001), Tropospheric ozone layers observed during PEM-Tropics B, *J. Geophys. Res.*, *106*, 32,527–32,538, doi:10.1029/2001JD900011.

Yoneyama, K., and D. B. Parsons (1999), A mechanism for the intrusion of dry air into the tropical western Pacific region, *J. Atmos. Sci.*, *56*, 1524–1546.

Zipser, E. J. (1977), Mesoscale and convective-scale downdrafts as distinct components of squall-line circulation, *Mon. Weather Rev.*, *105*, 1568–1589.

Zondlo, M. A., M. E. Paige, S. M. Massick, and J. A. Silver (2010), Development, flight performance, and calibrations of the NSF Gulfstream-V vertical cavity surface emitting laser (VCSEL) hygrometer, *J. Geophys. Res.*, *115*, D20309, doi:10.1029/2010JD014445.